TESTING A NOVEL HYBRID SPIRAL MICROPHONE ARRAY DESIGNED FOR PERFORMANCE AND PORTA

Matthew R. Aldeman
Illinois State University Department of Technology, Campus Box 5100, Normal, IL 61790
maldema@ilstu.edu

Jin Ho Jo
Illinois State University Department of Technology, Campus Box 5100, Normal, IL 61790
jjo@ilstu.edu

Abstract

In this investigation a novel hybrid spiral microphone array system is designed and constructed to maximize the overall performance of the array under the constraint that the array must be portable and capable of being transported in a small hatchback vehicle. Several microphone array designs are considered before settling on a modified Fermat spiral with microphones located exclusively on the axes of the array, enabling the array to be quickly disassembled into a small number of sections, transported to a remote location, and then re-assembled. The performance of the new microphone array is tested against an existing microphone array that was also designed for portability but with a more conventional logarithmic spiral design. The resolution of the new hybrid spiral array is found to greatly exceed the resolution of the conventional portable microphone array.

Introduction

A microphone array is a system of numerous spatially distributed individual microphones. The signals received by the system of microphones can be used to determine the location of an acoustic source through a process known as acoustic beamforming. In the past several decades, microphone array acoustic monitoring systems have become well known within the field of acoustics. However, until recently they have been practical only for well-funded research initiatives at corporate and government-funded laboratories due to their size and complexity. Because of this, single omnidirectional microphones remain the most common instrument to measure sound level. However, single omnidirectional microphones are unable to determine the location of an acoustic source. To incorporate directional information about the noise source, an array of microphones is necessary.

The primary reason that microphone arrays have historically been large and complex systems is because increasing the array diameter was the only means available to improve the angular resolution of the array. Throughout the mid-20th century, the Delay-and-Sum beamforming algorithm described by Johnson and Dudgeon [1] was the only algorithm in widespread use. Improved frequency-domain beamforming (FDBF) methods were developed in the 1980's using the Fast Fourier Transform [2]. In the past decade several advanced acoustic beamforming algorithms have been developed. These include a deconvolution method developed by Brooks and Humphreys [2] and an improved deconvolution method developed by Dougherty [3]. Even more recently, a method based on the spatial coherence of point sources and sidelobes in the frequency domain was developed by Sijtsma [4]. A similar method based on spatial coherence in the time domain was developed by Dougherty and Podboy [5]. These advanced algorithms allow for the development of smaller microphone arrays with performance levels that were not previously thought possible. These smaller, more affordable, and more portable arrays have the potential for widespread use across many disciplines. For example, a compact microphone array has been used successfully to identify and localize the sounds produced by small musical ensembles [6], the noise emitted by aircraft [7,8], and from wind turbines [9].

Although advanced beamforming algorithms have made it possible to achieve acceptable beamforming performance with smaller microphone arrays, it is still true that the best way to achieve high beamforming performance is to use large-diameter microphone arrays [10]. This is because of a principle known as the Rayleigh Criterion. It has long been accepted that the angular resolution of a microphone array system is approximated by the Rayleigh criterion, which indicates that angular resolution of the array is proportional to array diameter and inversely proportional to the signal's wavelength. This criterion was originally utilized in the field of optical imaging, but is also applicable to acoustics. However, the Rayleigh criterion is a convenient reference point rather than a fixed physical limit [11]. The Rayleigh resolution criterion defines the angular separation between two sources at the point where the maximum of the Airy disk (analogous to a diffraction pattern) of one source is located at the first minimum of the Airy disk of the second source. The Rayleigh criterion is given by:

$$W = \frac{rD}{\lambda z} \tag{1}$$

where *r* is the separation distance between the two sources, *D* is the diameter of the array, λ is the wavelength of the sources and *z* is the separation distance between the source and the array [12]. The Rayleigh criterion *W* is given by the first zero of the first-order Bessel function of the first kind, divided by a factor of pi to convert into radians. This results in a value of W = 1.22 for a circular, continuous aperture. If all else is held constant, then, the angular resolution performance of microphone arrays tends to increase with signal frequency and with the size of the array. Although the acoustic source frequency may be outside of the user's control, the diameter of the array can be controlled by the user because a user can choose the particular array for the application. This makes the diameter of the array one of the most important user-controlled parameters that govern the performance of the array. By using the Rayleigh criterion, a reasonable estimate of the angular resolution performance of an array can be made.

In addition to the overall diameter, the specific locations of the elements within the array influence the performance of the array. The layout of a typical array system has evolved gradually since the inception of array systems in World War 2. In the mid-20th century, one of the earliest applications of array systems was in the field of radio astronomy. The Mills Cross, which was a very large cross-shaped radio telescope, was constructed by Bernard Mills in Australia in 1954. The Mills Cross design utilized two perpendicular intersecting line segments, with sensors located at fixed intervals along each line segment. The Mills Cross array design has been widely used for both astronomical observation [13, 14] and acoustic localization [15, 16, 17]. The Mills Cross "X"-shaped array was used for several decades as the dominant design for microphone arrays. Today, the Mills Cross geometry is not a common configuration because of deficiencies in its design. Specifically, the configuration has many redundancies in the spacing distances between its elements. Thus, the design is not well-suited to beamforming operations across a wide range of frequencies because there are gaps where specific distances between elements are not represented in the array. Where these un-represented gaps correspond to specific wavelengths, the performance of the array and subsequent beamforming performance is poor [18]. (1)

In the 1990's, it was shown that a spiral-shaped array offered distinct advantages due to its lack of inter-element spacing distance redundancy. Robert Dougherty popularized a microphone array design that employed microphones arranged in a logarithmic spiral pattern. In contrast to the Mills Cross design, the advantage of a logarithmic spiral design is its inherent lack of repeated inter-element spacing distances. As a result, the beamforming results show reasonable performance over a wide range of source frequencies [16]. An example of a logarithmic spiral array design is shown in Fig. 1.

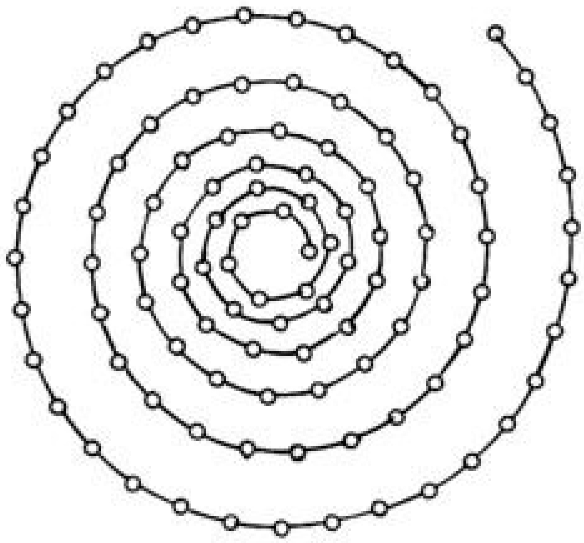

Fig. 1. Logarithmic Spiral Array. Source: [19]

A variety of other microphone array designs have been explored in the past several decades. For example, multi-arm spirals have become increasingly popular. Underbrink [20] proposed a multi-arm spiral array geometry as a way to spread the sensors more evenly in the angular dimension. Underbrink subsequently received a patent for a multi-arm elliptic logarithmic spiral microphone array design [21]. Malgoezar, Snellen, Sijtsma, and Simons developed another unique design approach by using a genetic algorithm to optimize the geometry of a microphone array [22]. They note that when the array is optimized for a particular frequency, the inter-element spacing distances asymptotically approach a constant value. However, the optimum inter-element spacing distance is completely dependent upon the signal frequency. Thus, an array designed for optimal performance at a particular frequency will be sub-optimal for a different frequency. To ensure reasonable performance over a wide range of frequencies, then, a large range of inter-element spacing distances should be used in the design of the array. As described earlier, this is the reason that spiral arrays tend to show reasonable performance across a wide range of frequencies.

It has become apparent to designers of microphone array systems that the spiral array design offers significant performance advantages across a wide frequency spectrum due to its lack of inter-element spacing redundancy. However, the drawbacks of the spiral design are the complexity of the design and the difficulty of scaling the design to larger dimensions. To achieve precise element placement, the sensor locations for a spiral array are typically machined with high-precision equipment such as CNC mills. More importantly, the design becomes unwieldy to transport as it is scaled to larger dimensions. For example, a small spiral array with a diameter of less than one meter is relatively portable, allowing it to be transported to various locations and used on a wide variety of test subjects. However, because the design cannot easily be broken down into discrete "legs" like the Mills Cross design and subsequently re-assembled at a test site, the spiral design cannot easily be scaled up to larger array diameters while maintaining portability. This is problematic because, as described earlier, angular resolution performance is proportional to the array diameter. Thus, both the spiral array and arrays with discrete legs like the Mills Cross array design feature distinct advantages and disadvantages. At the present time, a microphone array user must generally choose between these two fundamental design philosophies: microphone arrays generally offer either i. small diameter and high portability – typically using fixed microphone placements in shapes such as spirals – or ii. large diameter and low portability – typically using individual discrete microphone components that are individually re-positioned whenever the array is relocated.

Methodology

In previous work [18], the author explored four novel "hybrid" designs that address this fundamental microphone array design challenge. The purpose of the investigation was to create and test, in a controlled lab environment, a series of new microphone array designs that combine the benefits and mitigate the disadvantages of the two microphone array design philosophies described above. It was shown that the new "hybrid" design offered performance that was nearly as good as the spiral array, while offering portability and simplicity comparable to an array designed with independent legs which can be detached and re-attached. These performance characteristics were achieved by utilizing a spiral design, but changing the way the microphones are placed along the spiral arc. Instead of placing microphones at constant arc lengths along the spiral as in Fig. 1, microphones were placed at each point where the spiral intersects the horizontal or vertical axes. An example is shown in Fig. 2, where microphone locations are shown as red dots. The resulting array has microphones that are arranged exclusively on the axes, but the microphone separation distances are similar to a spiral array shape. This offers performance characteristics similar to the spiral array design, because array performance depends primarily on array diameter and the inter-element spacing distances between array elements (microphones). This design will also result in the array having two discrete legs, which will allow the array to be dis-assembled, transported to a new test location, and easily re-assembled. Because of the modular and easily-disassembled nature of this design, the overall diameter of the array when fully assembled can be increased, resulting in increased angular resolution performance.

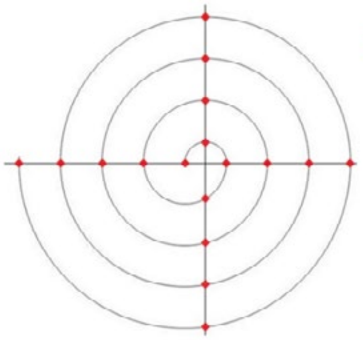

Fig. 2. Spiral with microphone locations at axis intersections

As a result of the author's previous work comparing four hybrid microphone designs in a lab environment [18], one hybrid microphone array design was selected for construction and testing in a real-world environment for the present investigation. The modified Fermat Spiral design was selected based on its performance, which was nearly as good as the baseline logarithmic spiral array. The array has 24 microphone elements and a diameter of 3.716 meters (146.3 inches). A diagram of the microphone placement is shown in Fig. 3.

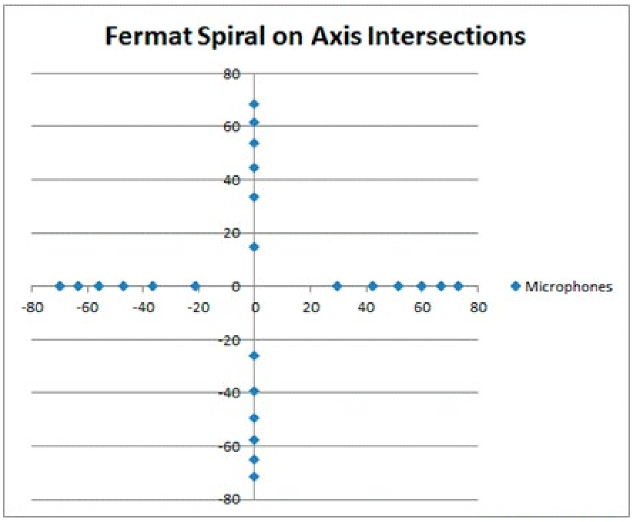

Fig. 3. Plot of microphone locations for Fermat Spiral Array with microphones at each axis intersection. All dimensions are in inches. Source: [18]

The fully constructed new hybrid spiral microphone array is shown in Fig. 4. The array can be quickly dis-assembled into four pieces: the two legs of the array, the "L"-shaped aluminum support piece at the base of the legs, and the wooden base at the bottom of the array, which is also attached with a hinge to the angle support. Each leg of the array is 216cm x 14cm x 7cm (85in. x 5 1/2in. x 2 3/4in.), the "L"-shaped aluminum base is 183cm x 7.6cm x 7.6cm (72in. x 3in. x 3in.), the wooden base is 122cm x 28cm x 3.8cm (48in. x 11 1/8in. x 1 1/2in.), and the wooden angled support piece is 132cm x 3.5cm x 3.5cm (52in. x 1 3/8in. x 1 3/8in.). Although the fully-assembled diameter of the array is 3.716 meters (146.3 inches), when dis-assembled the array can fit into the cargo area of a small hatchback vehicle (e.g. the author's Toyota Prius).

The microphone array consists of 24 electret condenser microphone circuits. The pressure signals received by each microphone pass through an amplifier circuit and the data is acquired with a MOTU 24 I/O 24-channel chassis. Each channel has 24-bit resolution, and the data is acquired at 44.1 kHz. The MOTU 24 I/O interfaces with a laptop computer equipped with recording software via USB connection. Data is acquired using dedicated studio-quality multi-channel recording software. The data is saved on the laptop for later processing using beamforming and image processing software. In addition to the microphones, the microphone arrays contain a video camera in the center of the array. The array's video camera interfaces directly with the laptop computer via USB connection. After the data analysis with the beamforming algorithms, the acoustic source maps can be displayed as an overlay on top of the video output. In this way, the location of the acoustic source may be clearly visualized.

(a)

(b)

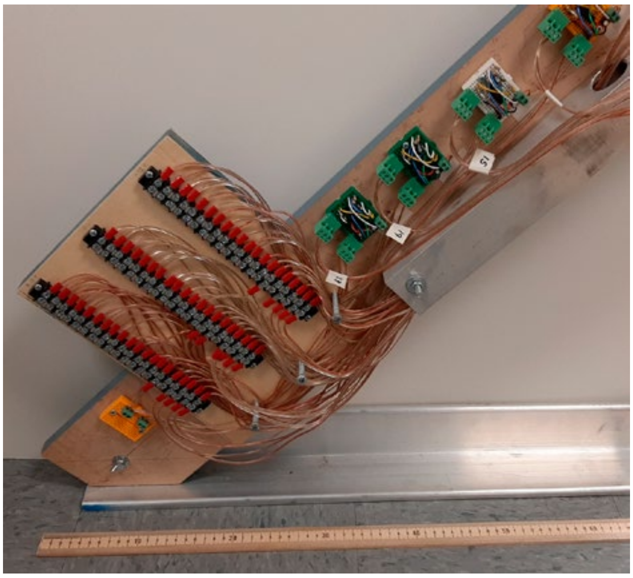

(c)

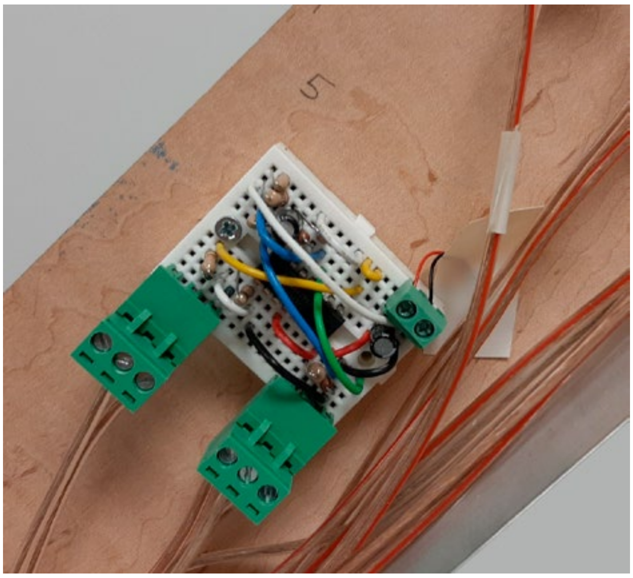

(d)

Fig. 4. (a) front view of the microphone array, (b) rear view, (c) rear view of one leg of the array showing power distribution and cable management, (d) one of 24 microphone signal amplifier circuits located on the rear of the array. A one-meter measuring stick is shown for reference.

To investigate the performance of the new microphone array, the array was run through the same test regimen as performed in the authors' previous work [6]. The array was used to record a small musical group (duet) consisting of a trombone and tenor saxophone playing a range of pitch intervals from unison up to two octaves. The results of the beamforming using the signals from the new array are compared to the results from the previous investigation that used a logarithmic spiral array with a diameter of 0.59 meters. The 0.59m logarithmic spiral array is an appropriate array for comparison because it was designed to be the largest logarithmic spiral planar array that could comfortably fit into the cargo area between the wheel wells of the same aforementioned hatchback vehicle. Thus, the two arrays offer roughly the same degree of portability. An image of the logarithmic spiral array that will be used for comparison is shown in Fig. 5.

Fig. 5. Baseline logarithmic spiral array with a diameter of 0.59m

Results

The test of the new hybrid microphone array consisted of recording two live musicians. One musician played the trombone at a concert pitch (233 Hz) throughout the experiment. The other musician played the tenor saxophone in an ascending chromatic scale, beginning with the first trial in unison and spanning two octaves up to a maximum of concert (932 Hz). The testing room is a large laboratory space with approximately 3.7m (12 ft.) ceilings tiled with acoustically absorbent ceiling tiles. To increase the acoustic absorbency of the surrounding lab, blankets were draped over walls and equipment in the surrounding area. The purpose of the experiment is to determine the ability of the array to identify the two discrete acoustic sources within the normal playing frequency range of the instruments. A summary of the test regimen is given in Table 1.

The video and 24-channel audio data from the experiment was saved on the laptop after each trial. After the recording session was complete, the data was processed with the Delay-and-Sum (DAS) beamforming algorithm. Although the DAS algorithm is one of the simplest beamforming algorithm available, it has the advantages of being computationally simple (making it fast to perform), it is widely recognized as a standard by which other algorithms are measured, and it is available on a range of platforms and applications. This makes it a good test case, because it is easily available to a wide audience.

The results of the beamforming algorithm are given in Fig. 6. The results from the 0.59m diameter logarithmic spiral baseline array are given in the left column, while the results from the new 3.716m hybrid spiral array are given in the right column. For convenient comparison, the musicians are playing the same notes in each row of Fig. 6.

In both columns of Fig. 6, the results show that the beamforming was successful at resolving two discrete sources in every case, although the two sources are not equally prominent in each case. When the acoustic sources do not appear to be the same size, this is caused by the amplitude of one source being slightly greater than the amplitude of the other source. In each case, the locations of the acoustic sources are identified reasonably accurately. Although the beamforming process seemed to correctly locate the acoustic sources in all cases, the least favorable results with the 0.59m logarithmic spiral array were obtained with the major 9th, major 10th, perfect 11th, and augmented 11th intervals. These correspond to images in Fig. 6(cc), (ee), (ii), and (kk). Part of the reason for the decreased performance at certain intervals is likely due to harmonic interference between the two acoustic sources, resulting in constructive or destructive interference as the frequencies are varied. This constructive or destructive interference could have an impact on the ability of the array system to distinguish between the two sources. However, the new hybrid spiral array did not show reduced performance at these intervals. In fact, the new hybrid spiral array showed greatly improved localization of the acoustic sources over every interval.

Interval Relationship	Musician 1 Note (Concert pitch)	Musician 1 Frequency [Hz]	Musician 2 Note (Concert pitch)	Musician 2 Frequency [Hz]	Corresponding Result
Unison	$B_3^\flat$	233	$B_3^\flat$	233	Fig. 6(a),(b)
Minor 2nd	$B_3^\flat$	233	B_3	245	Fig. 6(c),(d)
Major 2nd	$B_3^\flat$	233	C_4	262	Fig. 6(e),(f)
Minor 3rd	$B_3^\flat$	233	$D_4^\flat$	277	Fig. 6(g),(h)
Major 3rd	$B_3^\flat$	233	D_4	294	Fig. 6(i),(j)
Perfect 4th	$B_3^\flat$	233	$E_4^\flat$	311	Fig. 6(k),(l)
Augmented 4th	$B_3^\flat$	233	E_4	330	Fig. 6(m),(n)
Perfect 5th	$B_3^\flat$	233	F_4	349	Fig. 6(o),(p)
Augmented 5th	$B_3^\flat$	233	$G_4^\flat$	370	Fig. 6(q),(r)
Major 6th	$B_3^\flat$	233	G_4	392	Fig. 6(s),(t)
Minor 7th	$B_3^\flat$	233	$A_4^\flat$	415	Fig. 6(u),(v)
Major 7th	$B_3^\flat$	233	A_4	440	Fig. 6(w),(x)
Octave	$B_3^\flat$	233	$B_4^\flat$	466	Fig. 6(y),(z)
Minor 9th	$B_3^\flat$	233	B_4	494	Fig. 6(aa),(bb)
Major 9th	$B_3^\flat$	233	C_5	523	Fig. 6(cc),(dd)
Minor 10th	$B_3^\flat$	233	$D_5^\flat$	554	Fig. 6(ee),(ff)
Major 10th	$B_3^\flat$	233	D_5	587	Fig. 6(gg),(hh)
Perfect 11th	$B_3^\flat$	233	$E_5^\flat$	622	Fig. 6(ii),(jj)
Augmented 11th	$B_3^\flat$	233	E_5	659	Fig. 6(kk),(ll)
Perfect 12th	$B_3^\flat$	233	F_5	698	Fig. 6(mm),(nn)
Augmented 12th	$B_3^\flat$	233	$G_5^\flat$	740	Fig. 6(oo),(pp)
Major 13th	$B_3^\flat$	233	G_5	784	Fig. 6(qq),(rr)
Minor 14th	$B_3^\flat$	233	$A_5^\flat$	831	Fig. 6(ss),(tt)
Major 14th	$B_3^\flat$	233	A_5	880	Fig. 6(uu),(vv)
Perfect 15th	$B_3^\flat$	233	$B_5^\flat$	932	Fig. 6(ww),(xx)

Table 1. Summary of Testing Regimen

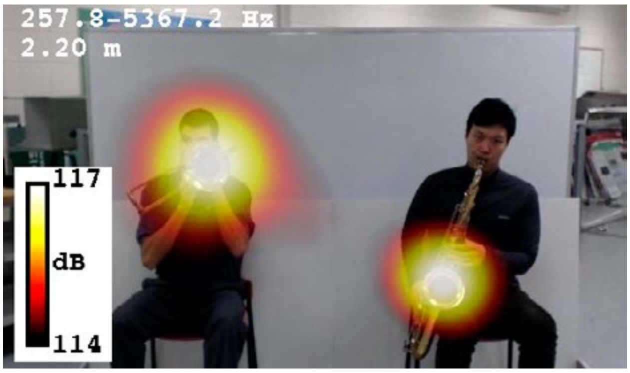
257.8-5367.2 Hz
2.20 m
117
dB
114

(a)


257.8-5367.2 Hz
2.20 m
110
dB
107

(b)


257.8-5367.2 Hz
2.20 m
117
dB
114

(c)


257.8-5367.2 Hz
2.20 m
111
dB
108

(d)


257.8-5367.2 Hz
2.20 m
119
dB
116

(e)


257.8-5367.2 Hz
2.20 m
114
dB
111

(f)

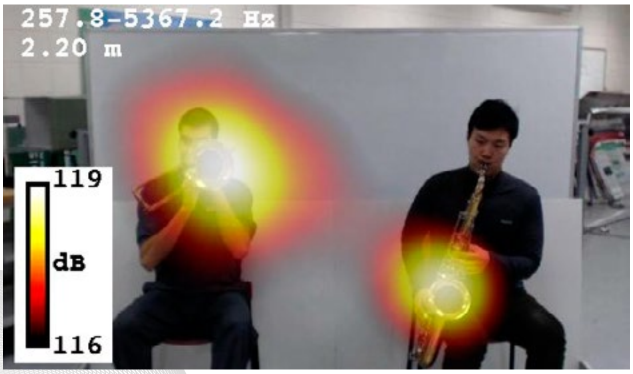
257.8-5367.2 Hz
2.20 m
119
dB
116

(g)


257.8-5367.2 Hz
2.20 m
114
dB
111

(h)

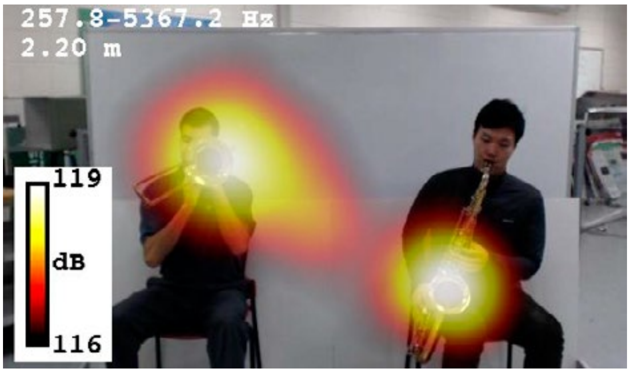
257.8-5367.2 Hz
2.20 m
119
dB
116

(i)


257.8-5367.2 Hz
2.20 m
113
dB
110

(j)

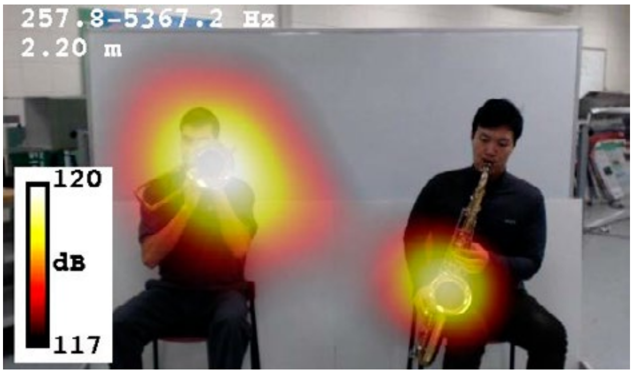
257.8-5367.2 Hz
2.20 m
120
dB
117

(k)


257.8-5367.2 Hz
2.20 m
112
dB
109

(l)

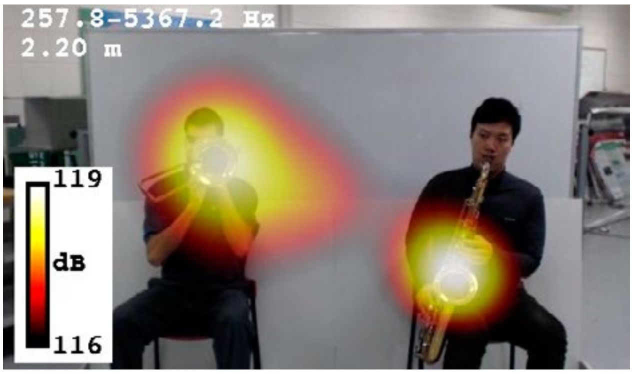
257.8-5367.2 Hz
2.20 m
119
dB
116

(m)


257.8-5367.2 Hz
2.20 m
112
dB
109

(n)

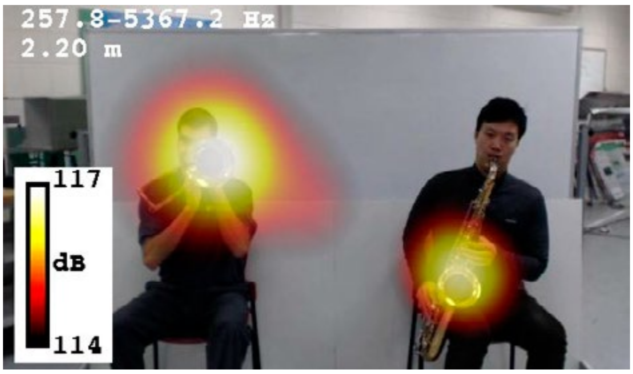
257.8-5367.2 Hz
2.20 m
117
dB
114

(o)


257.8-5367.2 Hz
2.20 m
109
dB
106

(p)


257.8-5367.2 Hz
2.20 m
117
dB
114
(q)


257.8-5367.2 Hz
2.20 m
112
dB
109
(r)


257.8-5367.2 Hz
2.20 m
118
dB
115
(s)


257.8-5367.2 Hz
2.20 m
111
dB
108
(t)

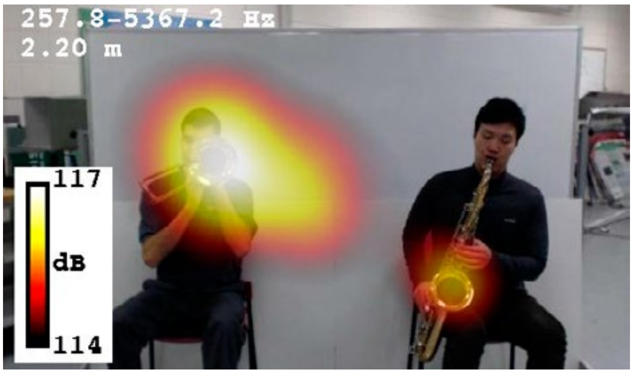
257.8-5367.2 Hz
2.20 m
117
dB
114
(u)


257.8-5367.2 Hz
2.20 m
112
dB
109
(v)

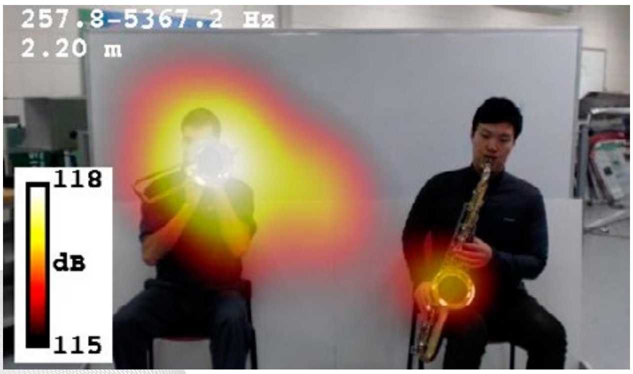
257.8-5367.2 Hz
2.20 m
118
dB
115
(w)


257.8-5367.2 Hz
2.20 m
115
dB
112
(x)

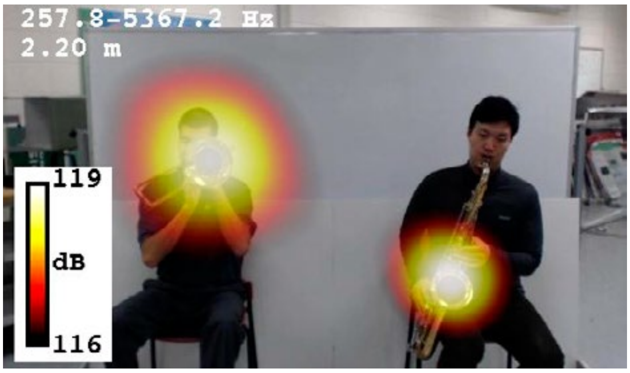

(y)

(z)

(aa)

(bb)

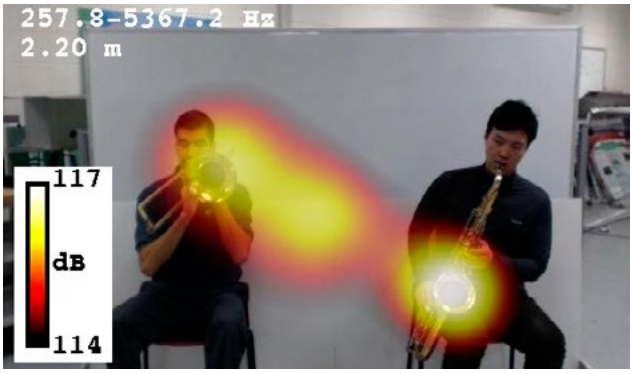

(cc)

(dd)

(ee)

(ff)

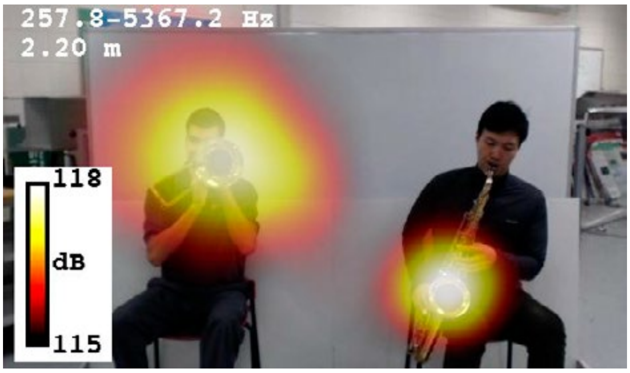

(gg)

(hh)

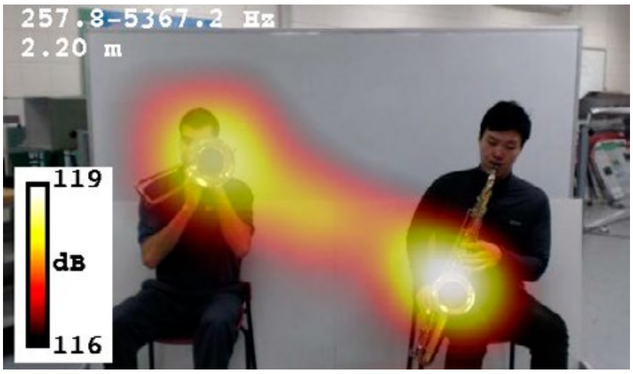

(ii)

(jj)

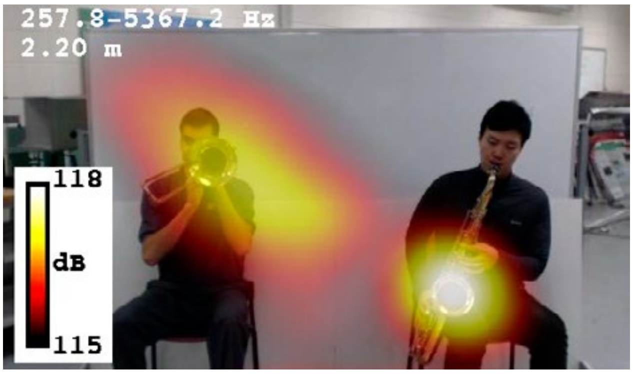

(kk)

(ll)

(mm)

nn)

(oo)

(pp)

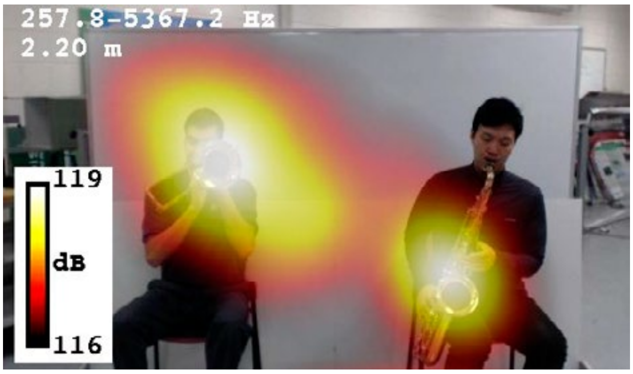

(qq)

(rr)

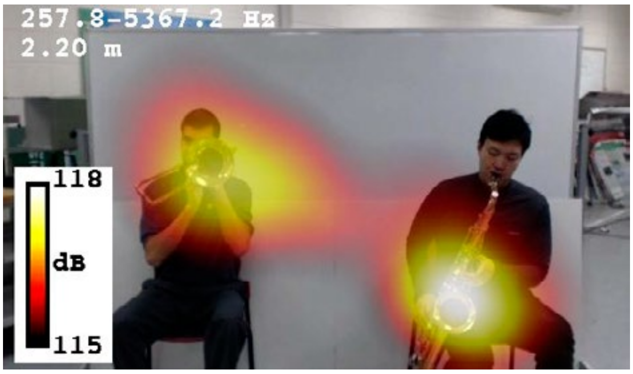

(ss)

(tt)

(uu)

(vv)

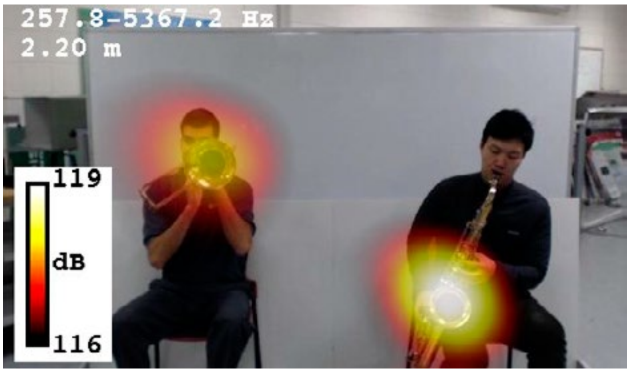

(ww)

(xx)

Fig. 6. Beamforming results. Each image corresponds to a beamforming result from an interval one half-step larger than the previous image. The pitch intervals for each image are given in Table 1.

Conclusion

This investigation demonstrated the performance of an innovative hybrid spiral microphone array design in a real-world environment. Based on prior lab testing in [18], the Fermat spiral with microphones placed at each axis intersection was selected for construction and implementation. The new microphone array combines the advantages of several other existing types of microphone arrays. It provides portability and convenience similar to a traditional spiral planar array, and it provides angular resolution performance that can typically be achieved only with a much larger array. The new array is designed specifically to be dis-assembled and stowed into the cargo area of a small hatchback vehicle.

For consistency and comparison with previous results, the new microphone array was tested with a small musical group in an identical environment to previous work [6]. Under the same test conditions, the beamform map produced by the new hybrid spiral array design was compared with the beamform map produced by a traditional spiral array that is similar in portability. The results of the beamforming analysis with the new microphone array show a beamform map that is much more precise than the baseline spiral array. This new array design can easily be taken to environments outside the laboratory and used for precise beamforming applications to identify the sources of acoustic sources, and will produce a beamform map that is more precise than a traditional planar microphone array of a size that is equally portable.

The testing regimen in this investigation was deliberately identical to previous work in order to directly compare the beamforming performance of the new microphone array design to an existing standard design. In the future, this work could be expanded by using a larger number of acoustic sources. For example, the array could be used to identify the acoustic sources in a larger ensemble such as a quartet or a small jazz ensemble. Alternatively, the array could be used to more accurately pinpoint the source of acoustic emissions from other sources such as automobiles or aircraft.

References

Johnson, D.H. & Dudgeon, D.E. Array Signal Processing: Concepts and Techniques. Prentice Hall. 1993.

T. F. Brooks and W. M. Humphreys, Jr. "A Deconvolution Approach for the Mapping of Acoustic Sources (DAMAS) determined from phased microphone array." J. Sound Vib. 294(4-5), 856–879, 2006.

R. P. Dougherty. "Extensions of DAMAS and Benefits and Limitations of Deconvolution in Beamforming." AIAA-2005-2961, 2005. 11th AIAA/CEAS Aeroacoustics Conference, Monterey, California, May 23-25, 2005.

P. Sijtsma. "CLEAN Based on Spatial Source Coherence." Int. J. Aeroacoustics, 6, 357–374, 2007.

R. P. Dougherty and G. Podboy. "Improved Phased Array Imaging of a Model Jet." AIAA-2009-3186, 2009. 15th AIAA/CEAS Aeroacoustics Conference (30th AIAA Aeroacoustics Conference), 11 - 13 May 2009, Miami, FL.

Aldeman, M.R., Jo, J.H. (2019). An Exploration of Compact Microphone Array Applications for Small Musical Groups. Akustika. Vol. 31 (March 2019), 153-163. https://www.journal6 akustika.com/journal/volume-31-2/

Chelliah, K., Raman, G., Aldeman, M. R., Patel, H. J. (2016). Demonstration of the Possibilities of Using a Phased Microphone Array as the Next-Generation Airport Noise Monitoring System. Transportation Research Record, 2600, 20-26 doi.org/10.3141/2600-03

Aldeman, M. R., Bacchus, R., Chelliah, K., Patel, H., Raman, G., Roberson, D. (2016). Aircraft noise monitoring using multiple passive data streams. Noise & Vibration Worldwide, 47(3-4), 35-45. 10.1177/0957456516663329

Ramachandran, R.C., Raman, G., and Dougherty, R.P. "Wind Turbine Noise Measurement using a Compact Microphone Array with Advanced Deconvolution Algorithms." Journal of Sound and Vibration 333 (2014) 3058-3080.

Aldeman, M. R., Raman, G. (2018). Effects of array scaling and advanced beamforming algorithms on the angular resolution of microphone array systems. Applied Acoustics / Elsevier, 132, 58-81. https://doi.org/10.1016/j.apacoust.2017.11.009

Aldeman, M. R., Raman, G. (2018) Experimental Determination of the Effects of Boundary Reflection on the Angular Resolution of Microphone Arrays. Building Acoustics/SAGE. Volume: 25 issue: 3, pp. 249-286. https://doi.org/10.1177/1351010X18768746

K. D. Möller. Optics. University Science Books. Mill Valley, CA. 1988.

B.Y. Mills and A.G. Little, "A high resolution aerial system of a new type," Austral. J. Phys., vol. 6, pp. 272-278, 1953.

M. Grill et al., "A new imaging riometer based on mills cross technique," in 7th International Symposium on Communication Theory and Applications, Ambleside, UK, 2003.

E.F. Berliner, J.P. Kuhn, S.A. Rawson and A.D. Whalen, "Acoustic Highway Monitor," U.S. Patent 6,021,364, issued Feb. 1, 2000.

R.P. Dougherty, "Beamforming in Acoustic Testing," in Aeroacoustics Measurements, T.J. Mueller, Ed. Berlin: Springer-Verlag Berlin and Heidelberg GmbH & Co. K, 2002, pp. 62-97.

G. McPherson et al., "Development of passive acoustic tracking systems to investigate toothed whale interactions with fishing gear," in ACOUSTICS 2004, Gold Coast, Aus, 2004.

Aldeman, M. (2020). A Hybrid Spiral Microphone Array Design for Performance and Portability. Applied Acoustics. Vol. 170 (15 December 2020). https://doi.org/10.1016/j.apacoust.2020.107512

R.P. Dougherty, "Spiral-shaped array for broadband imaging," U.S. Patent 5,838,284, issued Nov. 17, 1998.

J. Underbrink, "Aeroaoustic phased array testing in low speed wind tunnels," in Aeroacoustic Measurements, T.J. Mueller, Ed. Berlin: Springer-Verlag Berlin and Heidelberg GmbH & Co. K, 2002, pp. 98–217.

J.R. Underbrink, "Multi-arm elliptic logarithmic spiral arrays having broadband and off-axis application," U.S. Patent 6,583,768, issued June 24, 2003.

A. Malgoezar, M. Snellen, P. Sijtsma and D. Simons, "Improving Beamforming by Optimization of Acoustic Array Microphone Positions," presented at the Berlin Beamforming Conference, Berlin, 2016.

MATTHEW R. ALDEMAN

Matt Aldeman is an Associate Professor of Technology at Illinois State University in Normal, IL, USA, where he teaches in the Renewable Energy and Engineering Technology programs. Previously, he worked at General Electric as a wind site manager at the Grand Ridge and Rail Splitter wind projects. Matt is an honors graduate of the U.S. Naval Nuclear Power School and holds a B.S. in Mechanical Engineering from Northwestern University, a Master of Engineering Management from Old Dominion University, and a Ph.D. in Mechanical and Aerospace Engineering from the Illinois Institute of Technology. His research interests include acoustic localization techniques using microphone arrays and advanced beamforming algorithms, optimization of grid-connected renewable energy systems, Smart Grid technologies, and electric vehicles.

DR. JIN HO JO

Dr. Jin Ho Jo is a Professor of Technology at Illinois State University, teaching in the Sustainable and Renewable Energy program. Dr. Jo also leads the Sustainable Energy Consortium at the university. Dr. Jo is an honors graduate of Purdue University, where he earned a B.S. in Building Construction Management. He earned his M.S. in Urban Planning from Columbia University, where he investigated critical environmental justice issues in New York City. His 2010 Ph.D. from Arizona State University was the nation's first in sustainability. His research, which has been widely published, focuses on renewable energy systems and sustainable building strategies to reduce the negative impacts of urbanization.